PHYSICAL REVIEW D **85,** 034041 (2012)

Transverse strange quark spin structure of the nucleon

Tim Ledwig[1,*] and Hyun-Chul Kim[2,3,†]

[1]*Institut für Kernphysik, Universität Mainz, D-55099 Mainz, Germany*
[2]*Department of Physics, Inha University, Incheon 402-751, Korea*
[3]*School of Physics, Korea Institute for Advanced Study, Seoul 130-722, Korea*

(Received 14 October 2011; revised manuscript received 13 January 2012; published 27 February 2012)

We investigate the transverse quark spin densities of the nucleon with the lowest moment within the framework of the $SU(3)$ chiral quark-soliton model, emphasizing the strange quark spin density. Based on previous results of the vector and tensor form factors, we are able to determine the impact-parameter dependent probability densities of transversely polarized quarks in an unpolarized nucleon as well as those of unpolarized quarks in a transversely polarized nucleon. We find that the present numerical results for the transverse spin densities of the up and down quarks are in good agreement with those of the lattice calculation. We predict the transverse spin densities of the strange quark. It turns out that the polarized strange quark is noticeably distorted in an unpolarized proton.

DOI: 10.1103/PhysRevD.85.034041 PACS numbers: 13.88.+e, 12.39.−x, 14.20.Dh, 14.65.Bt

I. INTRODUCTION

The transversity of the nucleon is one of the most important issues in understanding the structure of the nucleon [1–3] (see also the reviews in [4–7]). However, because of its chiral-odd nature, it is challenging to determine it experimentally [4,8,9]. The processes discussed so far, to which the chiral-odd generalized parton distributions (GPDs) contribute, are: (hard exclusive) electroproduction of two vector- [10,11] or pseudoscalar mesons [12] and selected photoproduction reactions of lepton pairs [13] or of a pseudoscalar together with a vector meson [14]. Further promising processes, e.g. where the transversity distribution $h_1^q(x, Q^2)$ is accessed directly, are polarized proton-antiproton collisions [15–17], proposed by the PAX Collaboration [18]. The first experimental results on the transversity distribution $\delta q(x) = h_1^q(x, 0)$ were extracted in Refs. [19,20] through a combined analysis of data from the HERMES [21,22] and COMPASS [23] Collaborations on the SIDIS[1] process $lp^\uparrow \to l\pi X$ by using information on the Collins fragmentation function [24] provided by the Belle Collaboration [25]. On the theory side, chiral-odd GPDs were also investigated in various models [5,26–28].

Meanwhile, the QCDSF/UKQCD Collaborations have announced the first lattice results of the transverse spin structure of the nucleon [29], based on the work [30] that extended the analysis of Refs. [31,32] for the GPDs of the vector and axial-vector current to the generalized transversity distributions of the tensor current. In the present work, we investigate the transverse quark spin densities [30] of the nucleon with the lowest moment, using previous results for the nucleon vector and tensor form factors obtained within the $SU(3)$ chiral quark-soliton model (χQSM) [33–35]. In particular, we emphasize the transverse spin densities of the strange quark in the nucleon. The nucleon vector form factors were already computed within that framework in Refs. [36–38]. As a result, the strange vector form factors were predicted and turned out to be within the uncertainty of the experimental data [39]. The first calculation of the tensor charges of the nucleon in the χQSM has already been carried out many years ago [40,41]. The tensor form factors of the nucleon have been recently computed within the χQSM [42]. The results turn out to be similar to those of the lattice calculation. The strange tensor charge of the nucleon was also predicted in Refs. [41,42] and was found to be rather small. The anomalous tensor magnetic moments (ATMM) of the nucleon were computed in Ref. [43] within the same framework and were found to be positive and large for both up and down quarks as in the lattice calculation [29]. The ATMM plays an important role in describing the transverse deformation of the transverse polarized quark distribution in an unpolarized nucleon.

We use our previous results for these form factors and investigate them when viewed from the light front moving towards the nucleon. In this frame it is possible to extract spatial information on the nucleon, in which certain ambiguities arising from relativistic corrections are absent [31,32]. We will follow the strategy of the works [29,30,44,45] in $SU(2)$, where form factors obtained from lattice calculations and experimental data were used to map out nucleon transverse spin structures and transverse charge densities. We would also like to note the comprehensive investigations on generalized transverse momentum-dependent parton distributions [46,47] within the χQSM and the light-front constituent quark model, both in the three quark valence approximation. However, since we employ the $SU(3)$ version of the χQSM with explicit breaking of $SU(3)$ symmetry together with the

*ledwig@kph.uni-mainz.de
†hchkim@inha.ac.kr

[1]semi-inclusive deep inelastic scattering

whole Dirac sea, we are in a unique position to obtain spatial information on the transverse spin structure of the strange quark inside the nucleon.

II. TRANSVERSE QUARK SPIN DENSITIES

The vector and tensor form factors of the nucleon are defined in terms of the matrix elements of the vector and tensor currents, respectively,

$$\begin{aligned}
&\langle N_{s'}(p')|\,\bar{\psi}(0)\gamma^\mu\lambda^\chi\psi(0)|N_s(p)\rangle \\
&\quad = \bar{u}_{s'}(p')\left[F_1^\chi(Q^2)\gamma^\mu + F_2^\chi(Q^2)\frac{i\sigma^{\mu\nu}q_\nu}{2M_N}\right]u_s(p), \\
&\langle N_{s'}(p')|\,\bar{\psi}(0)i\sigma^{\mu\nu}\lambda^\chi\psi(0)|N_s(p)\rangle \\
&\quad = \bar{u}_{s'}(p')\left[H_T^\chi(Q^2)i\sigma^{\mu\nu} + E_T^\chi(Q^2)\frac{\gamma^\mu q^\nu - q^\mu\gamma^\nu}{2M_N}\right. \\
&\qquad \left. + \tilde{H}_T^\chi(Q^2)\frac{(n^\mu q^\nu - q^\mu n^\nu)}{2M_N^2}\right]u_s(p),
\end{aligned} \tag{1}$$

where γ^μ denotes the Dirac matrix and $\sigma^{\mu\nu}$ is the spin operator defined as $\sigma^{\mu\nu} = i[\gamma^\mu, \gamma^\nu]/2$. The λ^χ represent the Gell-Mann matrices, including the unit matrix $\lambda^0 = \sqrt{2/3}\mathbf{1}$. The ψ stands for the quark field and $u_s(p)$ designates the spinor for the nucleon with mass M_N, momentum p, and the third component of its spin s. The momentum transfer q and the total momentum n are defined as $q = p' - p$ with $Q^2 = -t = -q^2$ and $n = p + p'$. The form factors in Eq. (1) are related to the generalized form factors defined in Refs. [30,48] as follows: $F_1^\chi(Q^2) = A_{10}^\chi(t)$, $F_2^\chi(Q^2) = B_{10}^\chi(t)$, $H_T^\chi(Q^2) = A_{T10}^\chi(t)$, $E_T^\chi(Q^2) = B_{T10}^\chi(t)$, and $\tilde{H}_T^\chi(Q^2) = \tilde{A}_{T10}^\chi(t)$. Note that also the GPDs $H(x, 0, t)$, $E(x, 0, t)$, $H_T(x, 0, t)$, $E_T(x, 0, t)$ and $\tilde{H}_T(x, 0, t)$ are related to the form factors $F_1(t)$, $F_2(t)$, $H_T(t)$, $E_T(t)$ and $\tilde{H}_T(t)$ with the momentum fraction x integrated. We use the arguments of a given function to distinguish between GPDs, form factors and Fourier transformed form factors. Furthermore, we use the following normalizations and definitions for the proton flavor form factors $F_1^{u,d,s}$, the anomalous magnetic moment κ and the tensor anomalous magnetic form factor $\kappa_T(Q^2)$:

$$\begin{aligned}
&F_1^u(0) = 2, \quad F_1^d(0) = 1, \quad F_1^s(0) = 0, \quad \kappa = F_2(0), \\
&\kappa_T(Q^2) = E_T(Q^2) + 2\tilde{H}_T(Q^2),
\end{aligned} \tag{2}$$

with $\kappa_T = \kappa_T(0)$ as the ATMM. We want to mention that κ_T is a more important quantity than the two form factors E_T and $\tilde{H}_T$, since it is involved directly in describing the spatial distribution of the nucleon in the transverse plane.

The transverse spin densities of quarks with transverse polarization $\boldsymbol{s}$ in a nucleon with transverse spin $\boldsymbol{S}$ are expressed as [30]

$$\begin{aligned}
\rho(\boldsymbol{b}, \boldsymbol{S}, \boldsymbol{s}) = \frac{1}{2}\Bigg[& H(b^2) - S^i\epsilon^{ij}b^j\frac{1}{M_N}\frac{\partial E(b^2)}{\partial b^2} \\
& - s^i\epsilon^{ij}b^j\frac{1}{M_N}\frac{\partial\kappa_T(b^2)}{\partial b^2} \\
& + s^iS^i\left\{H_T(b^2) - \frac{1}{4M_N^2}\nabla^2\tilde{H}_T(b^2)\right\} \\
& + s^i(2b^ib^j - b^2\delta^{ij})S^j\frac{1}{M_N^2}\left(\frac{\partial}{\partial b^2}\right)^2\tilde{H}_T(b^2)\Bigg],
\end{aligned} \tag{3}$$

where $\boldsymbol{b}$ denotes the two-dimensional vector in impact parameter space with distance $b = \sqrt{b_x^2 + b_y^2}$ from the center of the nucleon momentum. The tensor ϵ^{ij} is an antisymmetric tensor with the property $\epsilon^{12} = -\epsilon^{21} = 1$. The operator ∇^2 is a Laplacian with respect to $\boldsymbol{b}$. The b^2-dependent form factors are given by the Fourier transformations of the vector and tensor form factors which are written generically as

$$\mathcal{F}^\chi(b^2) = \int_0^\infty \frac{dQ}{2\pi}QJ_0(bQ)F^\chi(Q^2), \tag{4}$$

where J_0 is a Bessel function with order zero. Note that the transverse quark spin densities in Eq. (3) are just the first moments of the two dimensional spin densities $\rho(x, \boldsymbol{b}, \boldsymbol{S}, \boldsymbol{s})$ that indicate the probability of finding a quark with momentum fraction x and transverse polarization $\boldsymbol{s}$ at distance b in a nucleon with polarization $\boldsymbol{S}$ [29,30].

III. FLAVOR VECTOR AND TENSOR FORM FACTORS OF THE NUCLEON

The vector and tensor form factors defined in Eq. (1) have been already studied in detail [36–38,42,43]. Since they are the basis of the present work, we will briefly recapitulate the results. We refer to Ref. [35] for a general formalism as to how to compute form factors within the χQSM. There are four different parameters in the χQSM: the cutoff mass Λ, the dynamical quark mass M, the current quark mass of the up and down quark $\bar{m}$, and the strange current quark mass. Apart from the dynamical quark mass M, all other parameters are fixed in the mesonic sector by using the pion decay constant $f_\pi = 93$ MeV, physical pion mass $m_\pi = 139$ MeV, and the kaon mass. Since various observables of the nucleon, such as the electric charge radii, are well reproduced with $M = 420$ MeV, we take this value as a fixed one. However, in order to show the dependence of the results on it, we will depict its dependence in shaded areas in figures with it varied between $M = 400$ MeV and $M = 450$ MeV.

The vector and tensor form factors $\mathcal{F}^q$ for the up, down and strange quarks ($q = u, d, s$) can be expressed in terms of flavor form factors $\mathcal{F}^\chi$ with $\chi = 0, 3, 8$:

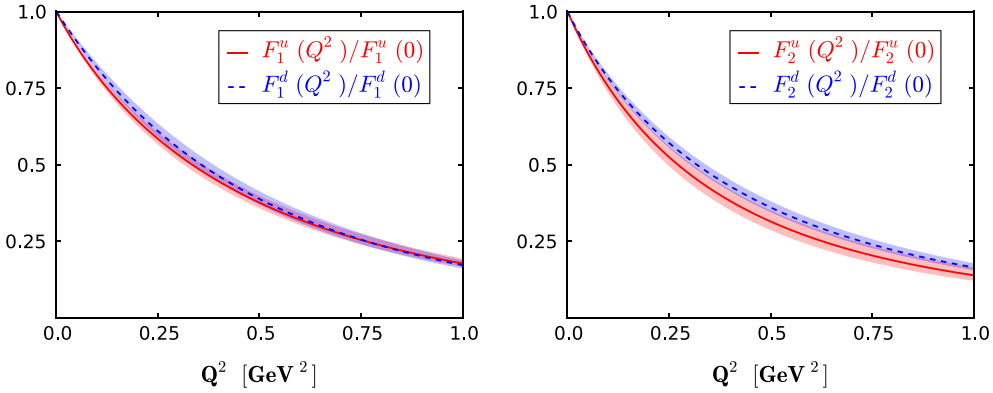

FIG. 1 (color online). Vector form factors of the proton for the up and down quarks from the χQSM. The values at $Q^2 = 0$ are $F_1^u(0) = 2$, $\kappa^u = 1.35$, $F_1^d(0) = 1$, and $\kappa^d = -1.80$. The anomalous magnetic moment of the proton is obtained as $\kappa_p = 1.49$ while the experimental value is $\kappa_p^{\mathrm{Exp}} = 1.79$. The curves correspond to the χQSM results with $M = 420$ MeV and the shaded areas to a variation of $M = 400$–450 MeV.

$$\mathcal{F}^u = \frac{1}{2}\left(\frac{2}{3}\mathcal{F}^0 + \mathcal{F}^3 + \frac{1}{\sqrt{3}}\mathcal{F}^8\right),$$
$$\mathcal{F}^d = \frac{1}{2}\left(\frac{2}{3}\mathcal{F}^0 - \mathcal{F}^3 + \frac{1}{\sqrt{3}}\mathcal{F}^8\right), \qquad (5)$$
$$\mathcal{F}^s = \frac{1}{3}(\mathcal{F}^0 - \sqrt{3}\mathcal{F}^8).$$

The vector form factors have been already studied in Refs. [36–38]. In particular, the strange vector form factors were predicted and turned out to be within the uncertainty range of the experimental data [39].

The left graph of Fig. 1 shows the proton up and down Dirac form factors as a function of Q^2 in solid and dashed curves, respectively. Note that they are normalized to one at $Q^2 = 0$ in order to compare their Q^2 dependences and look very similar to each other. In the right panel of Fig. 2,

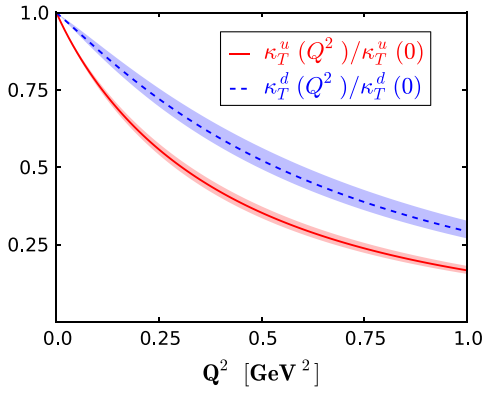

FIG. 2 (color online). Anomalous tensor magnetic form factors of the proton for the up and down quarks from the χQSM. The values at $Q^2 = 0$ are given as $\kappa_T^u = 3.56$ and $\kappa_T^d = 1.83$. The values of the lattice calculation are $\kappa_T^u = 3.70$ and $\kappa_T^d = 2.35$ at the scale of $\mu^2 = 0.36$ GeV^2 [29]. The curves correspond to the χQSM results with $M = 420$ MeV and the shaded areas to a variation of $M = 400$–450 MeV.

the up and down Pauli form factors are depicted, which are also normalized by the corresponding anomalous magnetic moments: $\kappa^u = 1.35$ and $\kappa^d = -1.80$ with $\kappa^u/\kappa^d = 0.75$. The experimental data for the proton and neutron anomalous magnetic moments, the $SU(2)$ approximation being considered, gives phenomenological values as $\kappa^u = 1.67$ and $\kappa^d = -2.03$ with $\kappa^u/\kappa^d = 0.82$. The anomalous magnetic moment for the proton is obtained as $\kappa_p = 1.49$, which is about 17% underestimated compared to the experimental data $\kappa_p^{\mathrm{Exp}} = 1.79$. The Pauli form factor for the up quark falls off faster than that for the down quark. Figure 2 shows the proton anomalous tensor magnetic form factors for the up and down quarks, respectively. The up form factor also decreases faster than the down form factor as Q^2 increases. We will see later that this difference will clearly appear in the transverse quark spin densities. In general, the χQSM shows the tendency that the slopes of the up quark form factors decrease faster than those of the down quark form factors. This implies that the up quark radii are smaller than those of the down quark so that the up quark seems to be located more to the center of the proton than the down quark.

In the lattice calculation [29], a simple p-pole parametrization for the tensor form factors

$$F(Q^2) = \frac{F_0}{(1 + Q^2/m_p^2)^p} \qquad (6)$$

was employed with the three parameters $F_0 = F(t = 0)$, m_p, and p for each form factor. The F_0 denotes the corresponding value of a form factor at $Q^2 = 0$ and m_p represents the p-pole mass in the unit of GeV. Similarly, we also utilize the parametrization of Eq. (6) for the vector and tensor form factors. In Table I, we list the numerical results of the parameters for the parametrization for each form factor.

Figure 3 draws the proton Dirac and Pauli form factor together with the anomalous tensor magnetic form factors

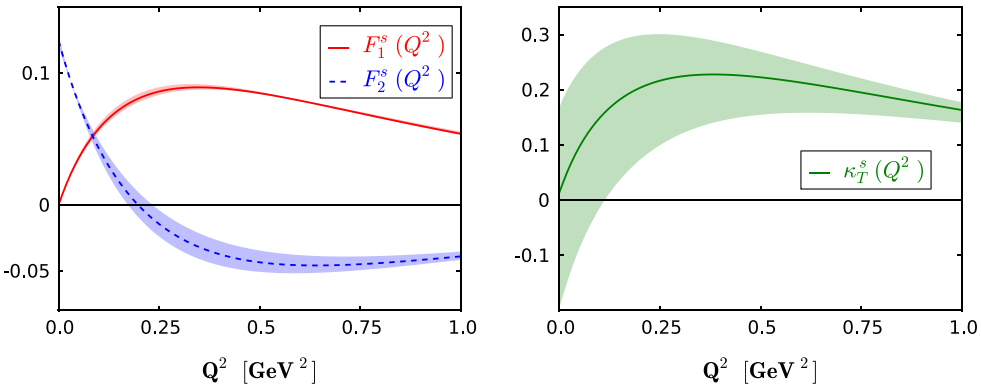

FIG. 3 (color online). Strange vector (left) and anomalous tensor magnetic (right) form factors of the proton from the χQSM with $M = 420$ MeV. The strange magnetic moment of the proton is obtained as $\mu_s = 0.12\mu_N$. The curves correspond to the χQSM results with $M = 420$ MeV and the shaded areas to a variation of $M = 400$–450 MeV.

of the strange quark. The strange quark Dirac form factor is naturally equal to zero at $Q^2 = 0$. The value of the strange quark Pauli form factor is the same as the strange magnetic moment of the nucleon: $\mu_s = 0.12\mu_N$ [37]. The strange quark ATMM is almost compatible with zero.

Both the strange quark Dirac and anomalous tensor magnetic form factors show Q^2 dependencies very similar to the electric form factor of the neutron. That is, they start to increase and then fall off slowly. On the contrary, the strange Pauli form factor decreases rather strongly until around $Q^2 \approx 0.25$ GeV^2 and as Q^2 increases, F_2^s gets larger. Moreover, F_2^s becomes negative from around $Q^2 \approx 0.2$ GeV^2. However, the general shape, multiplying the Pauli form factor by -1 and shifting it by a constant, is the same for all three strange quark form factors.

Because of this Q^2 behavior, it is not as simple as the case of the up and down form factors to parametrize the strange form factors. Thus, we introduce the following parametrization for the Fourier transform:

TABLE I. Parameters of the proton up and down form factors of the χQSM with $M = 420$ MeV fitted by the form $F(Q^2) = F_0/(1 + Q^2/m_p^2)^p$.

	F_1^u	F_2^u	κ_T^u	F_1^d	F_2^d	κ_T^d
p	2.72	2.65	2.43	5.62	3.02	5.70
$Q^2 = 0$	2	1.35	3.56	1	−1.80	1.83
m_p [GeV]	1.07	0.96	0.97	1.65	1.12	2.03

TABLE II. Parameters of the proton strange quark form factors from the χQSM with $M = 420$ MeV fitted in the form of $F(Q^2) = (a + bQ^2)e^{-cQ^{2d}}$.

	a	b	c	d
F_1^s	0	1.02	2.95	0.72
F_2^s	0.12	−0.63	2.59	0.81
κ_T^s	0.01	2.85	2.87	0.62

$$F(Q^2) = (a + bQ^2)e^{-c(Q^2)^d}, \tag{7}$$

where the four parameters a, b, c, and d are fitted to the form factors obtained from the χQSM. The corresponding values for each form factor are listed in Table II.

In general, we see that κ_T^s is the only form factor that shows a noticeable dependence on the constituent quark mass M. The values at $Q^2 = 0$ vary between -0.2–0.2 corresponding to the masses of $M = 400$–450 MeV. However, as Q^2 increases, the dependence on M gets milder and all the results have the same sign. In addition, since for Eq. (3) all form factors are multiplied by at least one power of Q in the Fourier transform, the uncertainty of the χQSM in $\kappa_T^s(0)$ does not affect much the transverse quark spin density calculation.

IV. RESULTS AND DISCUSSION

We now proceed to compute the transverse quark spin densities in a proton. We consider first unpolarized quarks in a transversely polarized nucleon with nucleon polarization $\boldsymbol{S} = (1, 0)$ and quark polarization $\boldsymbol{s} = (0, 0)$. We express these polarizations in the notation of $[\boldsymbol{S}, \boldsymbol{s}] = [(1, 0), (0, 0)]$. Afterwards we consider the unpolarized nucleon and transversely polarized quarks with $[\boldsymbol{S}, \boldsymbol{s}] = [(0, 0), (1, 0)]$. For these cases, the second line of Eq. (3) does not contribute to the spin densities. In the following discussion of the χQSM results, we use the constituent quark mass of $M = 420$ MeV and discuss at the end of this section a variation of $M = 400$–450 MeV.

In Fig. 4, we illustrate the transverse up and down quark spin densities of the nucleon. In the left panel we show the density of unpolarized up and down quarks in a transversely polarized nucleon for $[\boldsymbol{S}, \boldsymbol{s}] = [(1, 0), (0, 0)]$. As can be seen in Eq. (3), the deformation of these densities are governed by the Pauli form factors. We see that the down quark density is more distorted in the negative direction of b_y than the up quark density in the positive direction. The reason can be found in the fact that first the

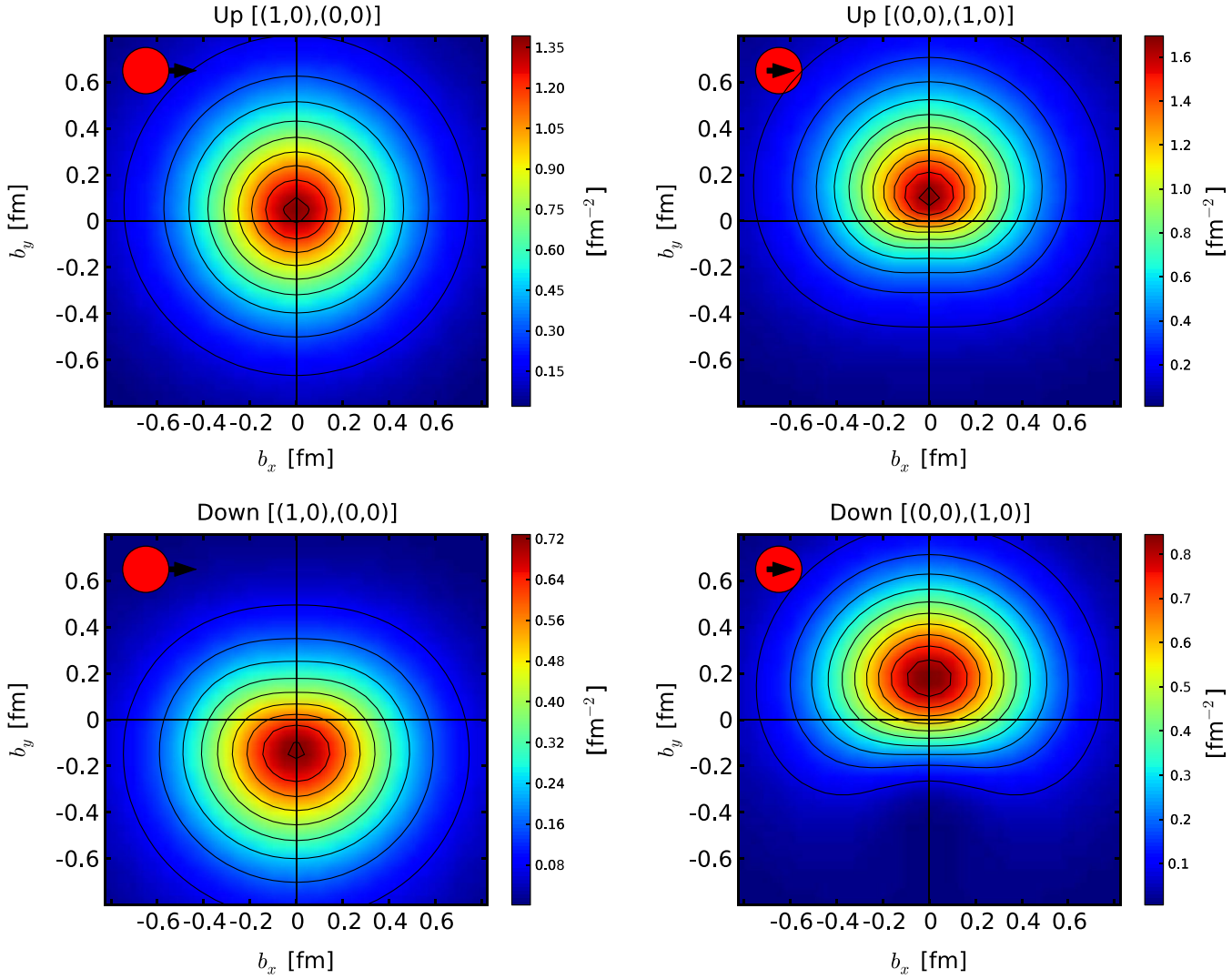

FIG. 4 (color online). Transverse up and down quark spin densities with the lowest moment of the nucleon from the χQSM with $M = 420$ MeV. In the upper left panel, the density of unpolarized quarks in a transversely polarized nucleon ($[\boldsymbol{S}, \boldsymbol{s}] = [(1, 0), (0, 0)]$) is drawn and in the upper right panel that of transversely polarized quarks in an unpolarized nucleon ($[\boldsymbol{S}, \boldsymbol{s}] = [(0, 0), (1, 0)]$). In the lower panel, we plot the down quark densities.

down Pauli form factor falls off more slowly than that of the up quark and second, the down anomalous magnetic moment ($\kappa^d = -1.80$) is negative. The sign of the form factors at intermediate Q^2 determines the direction of the shift. In the case of choosing the polarizations as $[\boldsymbol{S}, \boldsymbol{s}] = [(0, 0), (1, 0)]$, only the anomalous tensor magnetic form factors contribute, as shown in the right panel of Fig. 4. Because both κ_T^u and κ_T^d are positive, both transverse spin densities are deformed in the direction of positive b_y and again, because the form factor κ_T^d falls off more slowly, the density for the down quark is more strongly deformed. Furthermore, we want to mention that our results for the transverse up and down quark spin densities of the nucleon with the lowest moment are very similar to those from the lattice calculation [29].

Since both the strange Pauli form factor and anomalous tensor magnetic form factor turn out to be rather small, we can expect that the strength of the strange densities will be also quite small. Nevertheless, it is of great interest to see how much the transverse strange densities are distorted. Figure 5 plots the transverse strange quark spin densities with the lowest moment. Note that the magnitudes of the densities are smaller than those of the up and down quarks by an order of magnitude.

It is interesting to see that the density of unpolarized strange quarks in a polarized nucleon is negatively shifted. It is due to the fact that the strange Pauli form factor F_2^s turns negative from $Q^2 \approx 0.2$ GeV^2 and the lower Q^2 values are suppressed in the Fourier transform. Therefore, the negative values of the form factor at intermediate Q^2 shift the density

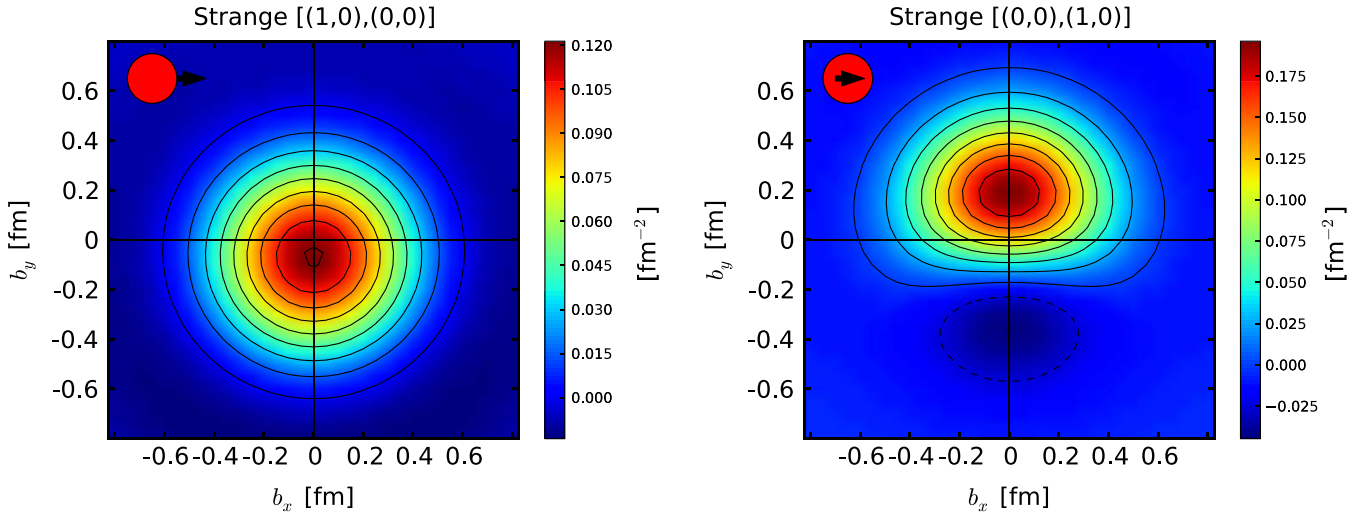

FIG. 5 (color online). Transverse strange quark spin densities of the nucleon from the χQSM with $M = 420$ MeV. In the left panel, the density of unpolarized strange quarks in a transversely polarized nucleon ($[\boldsymbol{S}, \boldsymbol{s}] = [(1, 0), (0, 0)]$) is drawn and in the right panel that of transversely polarized strange quarks in an unpolarized nucleon ($[\boldsymbol{S}, \boldsymbol{s}] = [(0, 0), (1, 0)]$).

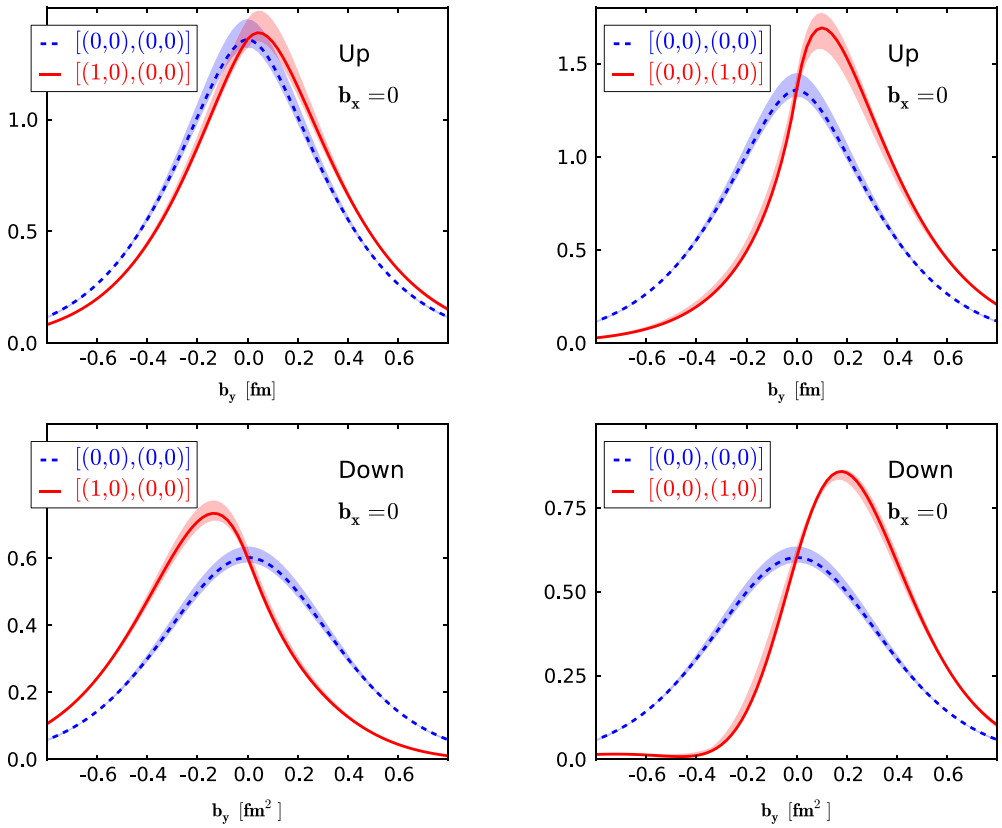

FIG. 6 (color online). Nucleon transverse up and down quark spin densities for $b_x = 0$ from the χQSM. In the upper left panel, the density of unpolarized quarks in a transversely polarized nucleon ($[\boldsymbol{S}, \boldsymbol{s}] = [(1, 0), (0, 0)]$) is drawn and in the upper right panel that of transversely polarized quarks in a unpolarized nucleon ($[\boldsymbol{S}, \boldsymbol{s}] = [(0, 0), (1, 0)]$). In the lower panel, we plot the down quark densities. The curves correspond to the χQSM results with $M = 420$ MeV and the shaded areas to a variation of $M =$ 400–450 MeV.

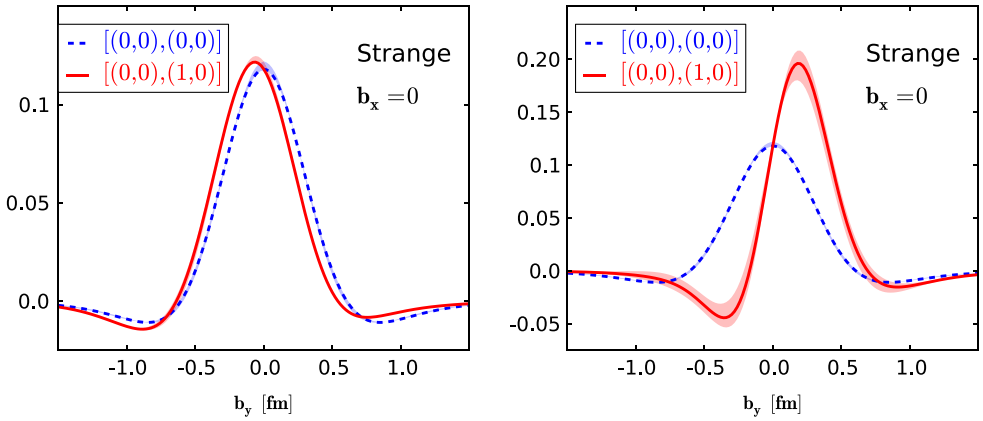

FIG. 7 (color online). Nucleon transverse strange quark spin densities from the χQSM for $b_x = 0$. In the left panel, the density of unpolarized strange quarks in a transversely polarized nucleon ($[\boldsymbol{S}, s] = [(1, 0), (0, 0)]$) is drawn and in the right panel, that of transversely polarized strange quarks in an unpolarized nucleon ($[\boldsymbol{S}, s] = [(0, 0), (1, 0)]$). The curves correspond to the χQSM results with $M = 420$ MeV and the shaded areas to a variation of $M = 400$–450 MeV.

to the negative b_y direction, despite the positive strange anomalous magnetic moment. On the contrary, the density of polarized strange quarks in an unpolarized nucleon is shifted and remarkably distorted in the direction of the positive b_y. This can be understood from the Q^2 dependence of $\kappa_T^s(Q^2)$ as shown in Fig. 3. Moreover, the density becomes negative for the negative values of b_y. One can see this later more clearly (see Fig. 7).

In Fig. 6 we draw the transverse up and down quark spin densities with b_x fixed to be zero. In the case of the unpolarized up quarks in a polarized nucleon, the density is slightly shifted to the positive direction of b_y, whereas that of the polarized up quarks in an unpolarized nucleon is quite much shifted to the positive b_y direction. Moreover, the width of the profile gets narrower and more peaked. On the contrary, the transverse down quark spin density for the unpolarized quarks in a polarized nucleon is changed to the negative b_y direction and shows an obvious distortion. That for the polarized quarks in an unpolarized nucleon is shifted to the positive b_y direction and distorted again.

Figure 7 shows the profiles of the transverse strange quark spin densities with $b_x = 0$. Interestingly, the density for the unpolarized strange quarks in a polarized nucleon is only slightly modified. In contrast, the polarized strange quarks are strongly redistributed in an unpolarized nucleon. As a result, the peak position is shifted to the positive b_y direction and becomes sharper. Moreover, the density becomes even more negative for the negative value of b_y than for the positive b_y.

In Figs. 6 and 7, we also depict the constituent quark mass dependence of our results. The curves correspond to the results with $M = 420$ MeV and the shaded areas to those with $M = 400$–450 MeV. These areas illustrate how the uncertainties in the form factor discussed in the last section influence the transverse spin densities. The form factor κ_T^s shows the most noticeable dependence on M, however, in the low Q^2 region only and the Fourier transform emphasizes the larger Q^2 region. As a result, the strange transverse spin densities depend mildly on M.

V. SUMMARY AND CONCLUSION

We investigated the transverse quark spin densities of the nucleon with the lowest moment, using the results of the vector and tensor form factors derived from the $SU(3)$ chiral quark-soliton model. We first recapitulated the flavor-decomposed anomalous vector and tensor magnetic form factors as functions of the momentum transfer. For numerical convenience, we made parametrizations of the form factors. Having combined these form factors and performed the Fourier transformations, we evaluated the transverse quark spin densities of the nucleon with the lowest moment. We considered two different cases, the density of unpolarized quarks in a polarized nucleon and that of polarized quarks in an unpolarized nucleon. The results turned out to be rather similar to the lattice QCD ones. Transversely polarized quarks in an unpolarized proton are both shifted to the positive direction of b_x. The shift is more prominent than the one occurring for unpolarized quarks in a polarized proton, where the density for the u quark is shifted to positive and that of the d quark to the negative b_y direction.

We presented in this work the first result of the transverse strange quark spin densities. Since the magnitudes of strange Pauli and anomalous tensor magnetic form factors are rather small, the strange densities turn out to be much smaller than those for the up and down quarks. However, the density for polarized strange quarks in an unpolarized

nucleon is noticeably distorted in the direction of the positive b_y and becomes more negative for the negative values of b_y.

In the present work, we considered only the transverse spin densities with the lowest moment. The generalized form factors with higher moments can be calculated in principle within the framework of the chiral quark-soliton model. However, we need to consider them carefully because of the presence of the derivative operators. The corresponding work is under progress. So far, we did not consider other cases of the transverse polarizations such as [(1,0), (1,0)] for which one requires information on the form factor $\tilde{H}_T$ and its derivative. However, we found that this form factor showed a numerically sensitivity. A related work addressing that is under way.

ACKNOWLEDGMENTS

H. Ch. K. is grateful to E. Epelbaum and M. V. Polyakov for their hospitality during his visit to Theoretische Physik Institute II in Ruhr-Universität Bochum, where part of the work was carried out. The authors are grateful to A. Metz for valuable comments and suggestions. The present work was supported by Basic Science Research Program through the National Research Foundation of Korea (NRF) funded by the Ministry of Education, Science and Technologyunder Grant No. 2010-0016265.

[1] J. P. Ralston and D. E. Soper, Nucl. Phys. **B172**, 445 (1980).
[2] R. L. Jaffe and X. D. Ji, Nucl. Phys. **B375**, 527 (1992).
[3] J. L. Cortes, B. Pire, and J. P. Ralston, Z. Phys. C **55**, 409 (1992).
[4] V. Barone, A. Drago, and P. G. Ratcliffe, Phys. Rep. **359**, 1 (2002).
[5] S. Boffi and B. Pasquini, Riv. Nuovo Cimento **30**, 387 (2007).
[6] Ph. Hägler, Phys. Rep. **490**, 49 (2010).
[7] G. A. Miller, Annu. Rev. Nucl. Part. Sci. **60**, 1 (2010).
[8] M. Diehl, T. Gousset, and B. Pire, Phys. Rev. D **59**, 034023 (1999).
[9] J. C. Collins and M. Diehl, Phys. Rev. D **61**, 114015 (2000).
[10] D. Y. Ivanov, B. Pire, L. Szymanowski, and O. V. Teryaev, Phys. Lett. B **550**, 65 (2002).
[11] R. Enberg, B. Pire, and L. Szymanowski, Eur. Phys. J. C **47**, 87 (2006).
[12] S. V. Goloskokov and P. Kroll, Eur. Phys. J. A **47**, 112 (2011).
[13] B. Pire and L. Szymanowski, Phys. Rev. Lett. **103**, 072002 (2009).
[14] M. El Beiyad, B. Pire, M. Segond, L. Szymanowski, and S. Wallon, Phys. Lett. B **688**, 154 (2010).
[15] A. V. Efremov, K. Goeke, and P. Schweitzer, Eur. Phys. J. C **35**, 207 (2004).
[16] M. Anselmino, V. Barone, A. Drago, and N. N. Nikolaev, Phys. Lett. B **594**, 97 (2004).
[17] B. Pasquini, M. Pincetti, and S. Boffi, Phys. Rev. D **76**, 034020 (2007).
[18] V. Barone (PAX Collaboration), arXiv:hep-ex/0505054.
[19] M. Anselmino, M. Boglione, U. D'Alesio, A. Kotzinian, F. Murgia, A. Prokudin, and C. Turk, Phys. Rev. D **75**, 054032 (2007).
[20] M. Anselmino *et al.*, Nucl. Phys. B, Proc. Suppl. **191**, 98 (2009).
[21] A. Airapetian *et al.* (HERMES Collaboration), Phys. Rev. Lett. **94**, 012002 (2005).
[22] L. Pappalardo for the HERMES Collaboration, *Tsukuba 2006, Deep Inelastic Scattering*, p. 667 (unpublished).
[23] E. S. Ageev *et al.* (COMPASS Collaboration), Nucl. Phys. **B765**, 31 (2007).
[24] J. C. Collins, Nucl. Phys. **B396**, 161 (1993).
[25] K. Abe *et al.* (Belle Collaboration), Phys. Rev. Lett. **96**, 232002 (2006).
[26] B. Pasquini, M. Pincetti, and S. Boffi, Phys. Rev. D **72**, 094029 (2005).
[27] H. Dahiya and A. Mukherjee, Phys. Rev. D **77**, 045032 (2008).
[28] M. Wakamatsu, Phys. Rev. D **79**, 014033 (2009).
[29] M. Göckeler *et al.* (QCDSF Collaboration and UKQCD Collaboration), Phys. Rev. Lett. **98**, 222001 (2007).
[30] M. Diehl and P. Hägler, Eur. Phys. J. C **44**, 87 (2005).
[31] M. Burkardt, Phys. Rev. D **62**, 071503 (2000).
[32] M. Burkardt, Int. J. Mod. Phys. A **18**, 173 (2003).
[33] D. Diakonov, V. Y. Petrov, and P. V. Pobylitsa, Nucl. Phys. **B306**, 809 (1988).
[34] D. Diakonov, in *Advanced School on Non-Perturbative Quantum Field Physics: Peniscola, Spain 2–6 June 1997*, edited by M. Asorey and A. Dobado (World Scientific, Singapore, 1998), p. 1.
[35] C. V. Christov *et al.*, Prog. Part. Nucl. Phys. **37**, 91 (1996).
[36] A. Silva, Ph.D. Dissertation, Ruhr-Universität Bochum (unpublished).
[37] A. Silva, H.-Ch. Kim, and K. Goeke, Phys. Rev. D **65**, 014016 (2001); **66**, 039902(E) (2002).
[38] A. Silva, H.-Ch. Kim, and K. Goeke, Eur. Phys. J. A **22**, 481 (2004).
[39] K. Goeke, H.-Ch. Kim, A. Silva, and D. Urbano, Eur. Phys. J. A **32**, 393 (2007).
[40] H.-Ch. Kim, M. V. Polyakov, and K. Goeke, Phys. Rev. D **53**, R4715 (1996).
[41] H.-Ch. Kim, M. V. Polyakov, and K. Goeke, Phys. Lett. B **387**, 577 (1996).

[42] T. Ledwig, A. Silva, and H.-Ch. Kim, Phys. Rev. D **82**, 034022 (2010).
[43] T. Ledwig, A. Silva, and H.-Ch. Kim, Phys. Rev. D **82**, 054014 (2010).
[44] C. E. Carlson and M. Vanderhaeghen, Phys. Rev. Lett. **100**, 032004 (2008); Eur. Phys. J. A **41**, 1 (2009).
[45] L. Tiator and M. Vanderhaeghen, Phys. Lett. B **672**, 344 (2009).
[46] C. Lorce, B. Pasquini, and M. Vanderhaeghen, J. High Energy Phys. 05 (2011) 041.
[47] C. Lorce and B. Pasquini, Phys. Rev. D **84**, 014015 (2011).
[48] Ph. Hägler *et al.*, Phys. Rev. D **68**, 034505 (2003).